Journal of Applied Geophysics 230 (2024) 105542

Contents lists available at ScienceDirect

Journal of Applied Geophysics

journal homepage: www.elsevier.com/locate/jappgeo

Insights from electrical resistivity tomography on the hydrogeological interaction between sand dams and the weathered basement aquifer

Hannah Ritchie [a], Ian Holman [a,*], Justus Nyangoka [a], Paul Bauman [b], Alison Parker [a]

[a] Cranfield Centre for Water, Environment and Development, Cranfield University, Bedford MK43 OTR, United Kingdom
[b] BGC Engineering, Inc, Calgary T2E 7W6, AB, Canada

ARTICLE INFO

Keywords:
Geophysics
Alluvial aquifer
Kenya
Drylands
Managed aquifer recharge

ABSTRACT

Sand dams, composed of recent alluvial aquifers behind concrete dam walls, are a water management technique in drylands. However, their level of hydraulic connectivity with their surrounding weathered basement aquifer is debated. This study aims to constrain this hydrogeological uncertainty in order to better understand their ability to meet water needs and improve dryland water security. The study is the first to use 2D geophysics (Electrical Resistivity Tomography) to provide evidence of seepage from sand dams at three mature and three newly built sites. A generally greater hydraulic connectivity was found between sand dams and their surrounding aquifer than has been assumed in some previous studies, with sites providing at least some local recharge rather than existing as isolated storage structures. This improved understanding is beneficial for both site selection and the performance of sand dams and can help ensure that maximum benefits are derived from the construction of a sand dam depending on its intended purpose.

1. Introduction

Drylands are defined by the Aridity Index as areas where the ratio of precipitation to potential evapotranspiration (P/PET) is <0.65 (Middleton et al., 1992). By the end of the 21st century they are predicted to become home to up to 5.2 billion people (Koutroulis, 2019), however, they possess only 8 % of global renewable water resources (Prăvălie, 2016). For current and future populations living in drylands, effective water management is, therefore, crucial for promoting sustainable livelihoods.

More than 70 % of the world's drylands are located in 'developing' countries (Safriel et al., 2005). Limited access to safely managed water in certain areas means that alternative improved water sources are essential to strengthen resilience. Water harvesting methods that collect and store surface water and/or increase the availability of groundwater are one such source. Sand dams, forming enhanced alluvial aquifers, which are recharged by streamflow, are one example (Maddrell, 2018).

Ephemeral rivers are common in drylands, with infiltration through such riverbeds considered an important pathway for recharging alluvial and basement aquifers (Philipp and Grundmann, 2013). Such recharge can be artificially increased by storing surface water to promote groundwater recharge to local aquifers (McCallum et al., 2013; Modie et al., 2022; Philipp and Grundmann, 2013). Studies on groundwater recharge in drylands have been conducted across the world, using techniques including stable isotope data, water table fluctuation models, monitoring wells, and chloride mass balance (Modie et al., 2022; Scanlon et al., 2006; Sorensen et al., 2024).

Sand dams are used on ephemeral rivers in drylands around the world. Sand dams store surface water and increase water availability for abstraction. However, there is uncertainty around their hydraulic connectivity with their surrounding aquifer (Hut et al., 2008; Yifru et al., 2021). Their relative importance for groundwater storage in the alluvium or recharge to the surrounding weathered basement aquifer is, therefore, contested.

Studies have modelled (Borst and Haas, 2006; Ndekezi et al., 2023; Quinn et al., 2019; Yifru et al., 2020), remotely sensed (Eisma and Merwade, 2021; Manzi and Kuria, 2011; Neufeld et al., 2021; Ryan and Elsner, 2016), or assumed (Eisma and Merwade, 2020; Hoogmoed et al., 2007; Hut et al., 2008; van Loon and Droogers, 2006; Maddrell, 2018; Quilis et al., 2009) seepage of water from sand dams laterally into the weathered basement and longitudinally under or around the dam wall. Hut et al. (2008) found the impact of sand dams on groundwater levels in riverbanks directly upstream of the dam walls to range from 70 to 80 m into the riverbanks. The sub-vertical component of lateral seepage

* Corresponding author.
E-mail address: I.holman@cranfield.ac.uk (I. Holman).

https://doi.org/10.1016/j.jappgeo.2024.105542
Received 10 January 2024; Received in revised form 2 October 2024; Accepted 11 October 2024
Available online 13 October 2024
0926-9851/© 2024 The Authors. Published by Elsevier B.V. This is an open access article under the CC BY license (http://creativecommons.org/licenses/by/4.0/).

into the underlying weathered basement via the river channel base, which is especially difficult to monitor, is usually either assumed (Eisma and Merwade, 2020; Maddrell, 2018; Quinn et al., 2019) or discounted (Ertsen et al., 2005; Nissen-Petersen, 1997).

Whilst sand dams can be constructed to serve different purposes of storage or recharge, their hydraulic connectivity with their surrounding environment is rarely explored pre-construction. This general uncertainty is, therefore, the basis for this research. The study aims to determine to what degree sand dams are losing water laterally (and sub-vertically) and longitudinally into the surrounding aquifer and downstream respectively. Studies in similar dryland environments have utilised geophysical techniques to investigate hydrogeological connections between alluvium and underlying crystalline basement (Issoufou Ousmane et al., 2023). This study therefore sought to contribute to this existing knowledge in the specific context of sand dams, being the first to use 2D geophysics at sand dam sites and to collect field-based data before and after sand dam construction. It therefore aims to provide novel evidence on whether sand dams generally exist more as storage or Managed Aquifer Recharge (MAR) structures.

2. Methods

2.1. Study area

The study took place at six sites in the north and south of Makueni County, Kenya (Fig. 1) across semi-arid and dry sub-humid regions (0.2 < P/PET <0.65) (UNEP-WCMC, 2007). Average annual precipitation from 1981 to 2022 at the six sites varied between 586 and 797 mm at the southern and northern sites respectively (CHIRPS-GEFS Precipitation Forecasts, 2021) (Fig. 1). The northern sites are at a higher elevation of >1100 m asl, whilst the southern sites are at <850 m asl and are in slightly less incised valleys. The catchment size for each site is similarly small, with the largest measuring approximately 72 km^2.

Three mature sand dam sites: Kithunthi, Kipico, and Ngulai (constructed in 2016, 2016, and 2013 respectively), and three new sites: Nthonzweni, Wambiti, and Kyakivandi (constructed in 2022) were studied. Kipico and Ngulai were selected because of available data from Quinn et al. (2019) who conducted a water balance to assess flow rates at three sand dams. Their third site was not selected due to rocky ground conditions that were unsuitable for the use of geophysical equipment. A third mature site (Kithunthi) was selected based on suitable ground conditions, telemetered data indicating prolonged water storage, available abstraction data, and reasonable accessibility from the other sites. The three new sites were selected due to planned construction during the 2022 fieldwork period, suitable ground conditions, and reasonable accessibilty from the mature sites.

2.1.1. Geological and hydrogeological setting

The sites, in common with much of the Basement Complex geology across approximately 34 % of Africa are predominantly composed of granitoid and biotite gneiss, with some minor schist (Baker, 1952; Dodson, 1953; MacDonald and Calow, 2009). Subject to weathering, Precambrian basement rocks can establish a weathered profile typically comprising residual soil and saprolite, together forming the regolith, and saprock and fresh, unweathered bedrock, together forming the crystalline bedrock (Bianchi et al., 2020; Rusagara et al., 2022; Wright and Burgess, 1992; Zarate et al., 2021) (Fig. 2). Aquifers can form either in the primary porosity of river alluvium or in the secondary porosity of the underlying weathered bedrock (Bakundukize et al., 2016; Elster et al., 2014; Wright and Burgess, 1992). Typically, the saprolite has a predominantly storage function and the saprock a transmissive one (Bakundukize et al., 2016; Elster et al., 2014) (Fig. 2).

The base of the alluvium is at the interface between surface and groundwater flow (Brunner et al., 2017). The alluvial sand dam aquifer and groundwater in the weathered basement below can be either hydraulically connected or disconnected, largely depending on the nature of the saprolite and climatic conditions (Watson et al., 2021; Wright and Burgess, 1992). During sufficient rainfall, surface and groundwater systems in drylands can be connected (Watson et al., 2021). If the saprolite is very clay-rich and therefore relatively impermeable, any water stored in the alluvial riverbed may form a pseudo-perched aquifer, with an aquiclude limiting flow to the underlying groundwater.

In the dry season, the depth to the water table often prevents discharge along the river channel. Through the water stored in the alluvium after the construction of a sand dam, the water table is locally raised in the riverbed (Fig. 3). This creates a groundwater mound (Borst

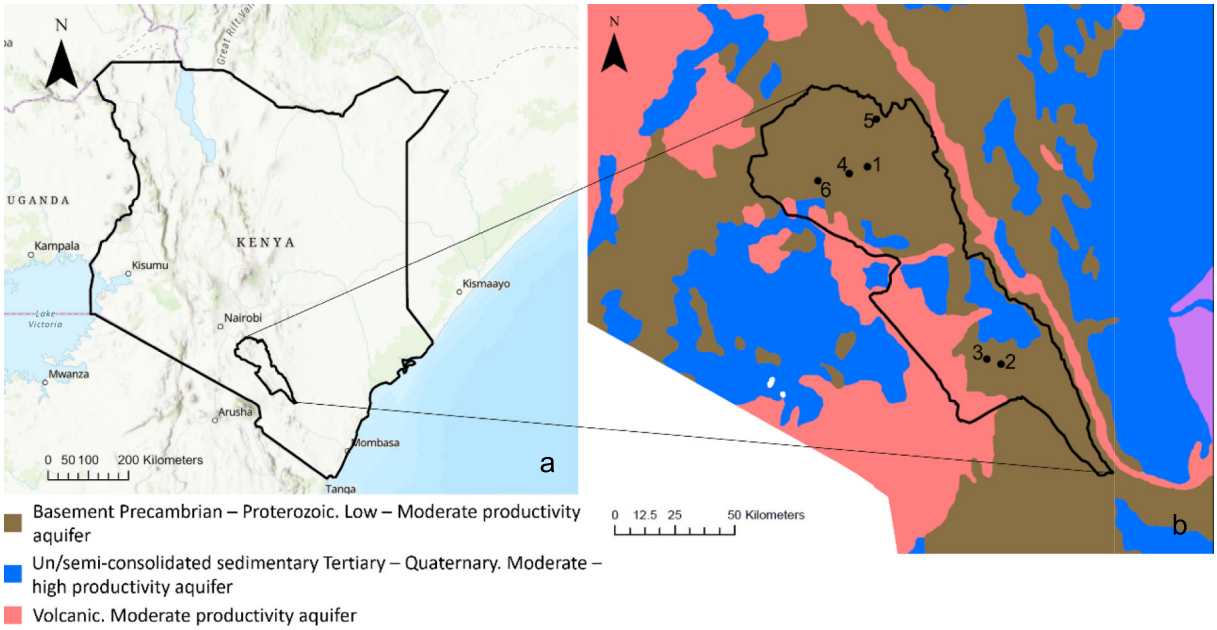

Fig. 1. (a) Map of Kenya with Makueni county inset, (b) geological and hydrogeological map of Makueni County, Southeast Kenya indicating aquifer productivity (British Geological Survey, 2024) and study sites: (1) Kithunthi; (2) Kipico; (3) Ngulai; (4) Nthonzweni; (5) Wambiti; (6) Kyakivandi. Reproduced with the permission of the British Geological Survey © UKRI [2024]. All Rights Reserved.

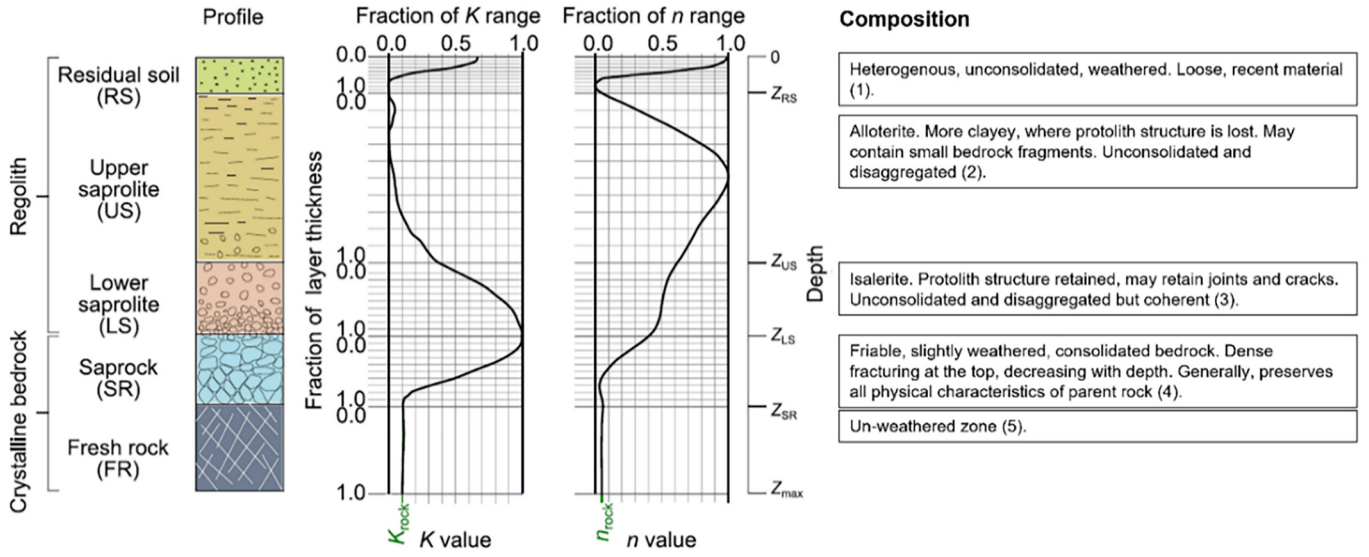

Fig. 2. Conceptual model of physical heterogeneity in a weathered basement aquifer, highlighting K (hydraulic conductivity) and n (porosity) (Adapted from Bianchi et al., 2020 under the CC BY 4.0 licence. Contains British Geological Survey material © UKRI 2020) and typical compositions. (1) (Bakundukize et al., 2016; Kayode et al., 2022). (2) (Ulusoy and Kadioğlu, 2021). (3) (Wright and Burgess, 1992). (4) (Wright and Burgess, 1992). (5) (Bianchi et al., 2020).

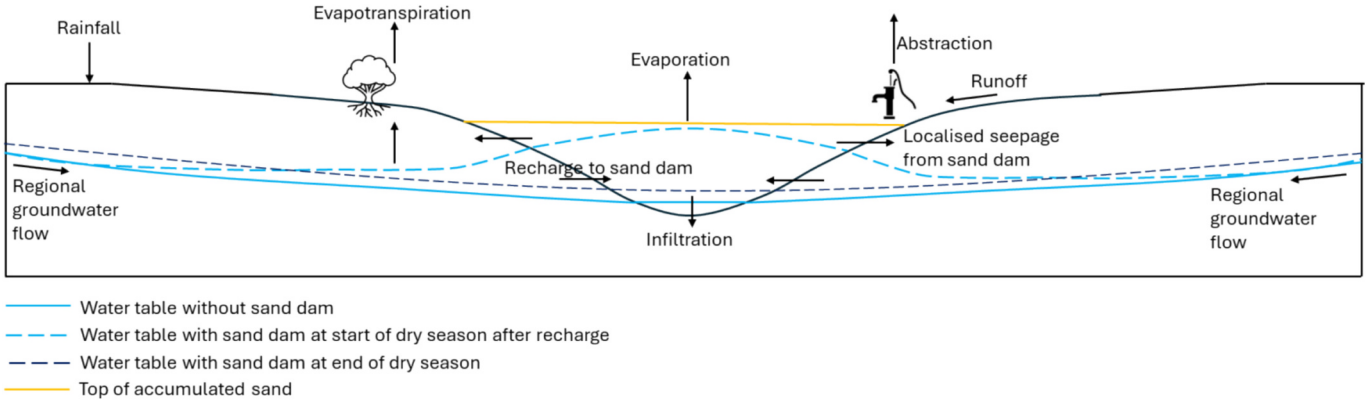

Fig. 3. Conceptualisation of the impact of a sand dam on water levels in the riverbed and surrounding riverbanks based on previous studies (Borst & Haas, 2006; Strohschein, 2016).

and Haas, 2006; Strohschein, 2016), where the water table is higher than in the adjacent riparian zone, allowing water to seep from the alluvium into the surrounding aquifer. This water can recharge the water table in the weathered basement until equilibrium is reached if there is a connection between the two. Some water in the riparian zone is hypothesised to be lost to evapotranspiration by surface vegetation (Strohschein, 2016; Yao et al., 2018).

2.2. Data collection

2.2.1. Field studies

Two field studies in Kenya were conducted in February–March 2022 and 2023. The fieldwork involved geophysical surveys using ERT and Induced Polarisation (IP), and field observations.

Electrical resistivity (called resistivity from here) methods are used to identify geological structures by proxy due to differences between resistivity values of subsurface materials (Lowrie, 2007). ERT is a 2D multi-electrode geophysical method that relies on an injection of current and the response of voltage to measure a material's resistivity. IP can be collected during the same measurement cycle and measures a material's chargeability. In theory, it can help to differentiate between clay and water, which both have low resistivity values, whilst the former has much higher IP values (Shao et al., 2021). For a detailed description of the ERT and IP techniques, refer to Loke (1999) and Lowrie (2007) respectively. ERT was chosen over other geophysical methods due to its common use and merit in groundwater studies, its sensitivity to both lithology and water content, and its 2D capabilities (Ebong et al., 2021; Kumar et al., 2016; Saad et al., 2012).

An ABEM Terrameter LS resistivity meter was used to collect the ERT data. Two array types: Gradient and Schlumberger, were used to investigate repeatability of results. Two cables and 41 electrodes were used in each profile. Salt water was added around the electrodes to improve ground contact due to soil aridity.

Between four and five main profiles were undertaken at each site (Error! Reference source not found.) to assess lateral and longitudinal seepage, and the composition of the underlying weathered basement. In 2022 three profiles parallel to the dam wall were taken at each site. These included one downstream, one far enough upstream to avoid interference from metal reinforcement in the dam wall, and one 95–150 m upstream to be within the calculated range of sediment accumulation but at least 90 m from profile 2 to assess whether a difference was visible (Fig. 4, (profiles 1–3 respectively)). One profile perpendicular to the dam wall in the middle of the riverbed (Error! Reference source not found., (profile 4)) was undertaken at all six sites. Profiles 1 and 2 were

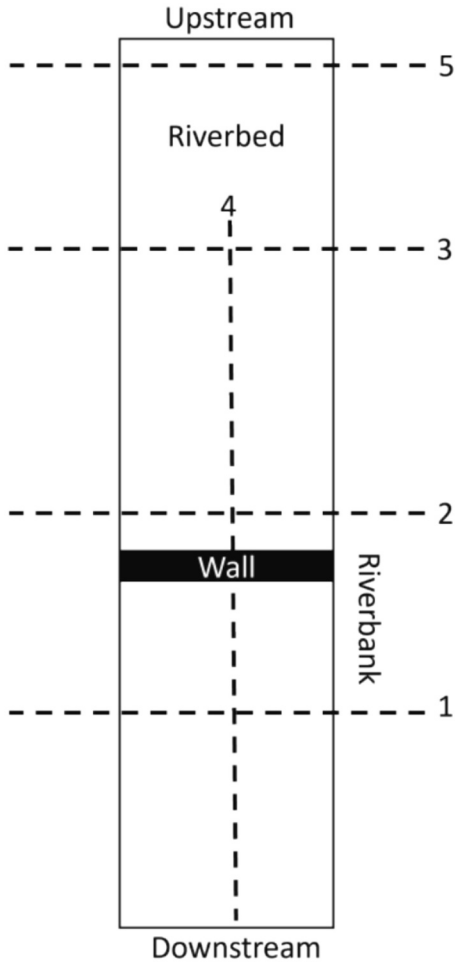

Fig. 4. ERT profile locations. Profiles 1–3 (parallel) and 4 (perpendicular) were conducted at all sites. Profile 5 was conducted only at Kipico. See Supplementary Material for specific dimensions.

generally within 20 m of the dam wall to capture impact of seepage downstream and to compare near-dam wall conditions with those conditions far upstream in profiles 3 and 4. Profile 5 located 500 m upstream was performed only at Kipico to assess whether water levels differ upstream of the accumulated trapped alluvium (that which has built up since dam wall construction). Profile locations were sometimes constrained by construction activities at new sites, as well as rock outcrops and roads.

In 2023, these profiles were repeated at Kithunthi to assess reproducibility and at the new sites to compare differences pre- and post-dam construction. Surface water upstream of the dam walls at Wambiti and Kyakivandi in 2023 meant that perpendicular profiles could not extend upstream of the walls here.

Profiles used a minimum electrode spacing of 4 or 5 m, giving profiles of between 160 and 200 m in length and up to 30 m in depth. IP data were collected alongside resistivity data at all of the 2023 profiles using the Schlumberger array. The Schlumberger and Gradient arrays gave similar resistivity inversion profiles. Whilst both were used to aid interpretation, the results report only the gradient arrays. All profiles are included in Supplementary Material.

To help in making the hydrogeological interpretations of the geophysical inversions, a series of observations and measurements were taken. These included groundwater level measurements in the alluvium and riverbed (Table 5), probing to help in truthing the depth of the alluvial deposits, soil profiles, topographical profiles, surface geological observations of rock type and degree of weathering, and irrigation surveys (Supplementary Material). Irrigation surveys with all available plot owners were used to understand where irrigation may have increased water content in the geophysics profiles for reasons other than rainfall or water loss from the dams.

2.2.2. Literature review

Resistivity values from published studies for each of the layers found in the weathered basement were used to help in truthing the ERT inversions in this study (Table 1). Values of each material were taken from studies conducted in basement aquifers with at least some gneiss due to its dominant presence in the study sites.

Resistivity values can vary greatly for several reasons, making it difficult to determine the most significant contributor to bulk resistivity. Higher resistivity in the regolith is often characteristic of dry, compact sand, gravelly sand, or laterite (Anudu et al., 2014; Kayode et al., 2022). Lower values can be associated with a combination of higher water, clay, mineral salt, soil organic content, or porosity (Anudu et al., 2014; Kayode et al., 2022; Nyenje et al., 2022). The resistivity of saprock generally increases with depth as fracture density decreases as the occurrence of fluids decreases. Furthermore, fractures filled with water or decomposed clays from the saprolite can create heterogeneities in resistivity values in the saprock (Elster et al., 2014; Zarate et al., 2021). Finally, resistivities of fresh bedrock are greater than weathered rock (Shao et al., 2021), and can be impacted by mineral composition (Matsui et al., 2016), which can be affected by the degree of metamorphism (Bakundukize et al., 2016).

2.3. Data analysis

Raw data were cleaned in LS toolbox. Data points with a variance of >1 % were removed, followed by any data points with a voltage of <0.0015 V, based on standard cleaning procedures (J. Adcock, personal communications, January 2022). A median of 2.9 % of data points were removed from profiles. Data were inverted in Res2Dinv to give a resistivity section (Kayode et al., 2022). 'Bad data points' (i.e., those with very high, very low or negative apparent resistivities) were exterminated. In the inversion settings a damping factor of 0.3 was generally used due to challenging electrode contact associated with the aridity of the ground (Loke, 1999). The robust-constraint least squared method was chosen to avoid a smearing effect between the regolith and bedrock (Elster et al., 2014) and due to lower errors produced with this method. During inversion, the stop criteria was set with a 5 % error reduction. A maximum of 6 iterations were carried out so that the difference between the model response and measured data was minimal but results were not unrealistic. Regular contour intervals were used for each profile, with a minimum of 5 Ω.m and a maximum of 3000 Ω.m.

3. Results

Resistivity inversions supported by IP, surface observations, and literature provide insight into lateral and longitudinal seepage from sand dam alluvial aquifers into the surrounding weathered basement, indicating their level of hydrogeological interaction.

3.1. Geology of sand dams and their surrounding aquifer

The results from all six sites confirm that at least some of the trapped alluvium behind a sand dam wall is underlain by weathered basement material that is consistent with Fig. 2. The resistivity and thickness ranges of the five layers (alluvium in the riverbed, residual soil in the riverbanks, saprolite, saprock, and fresh bedrock) are outlined in Table 2. The thickness of each layer varies along the river channel and between sites, indicating variable degrees of weathering of the underlying protolith, which can impact the water storage potential of sites.

Table 1
Resistivity ranges of each material in a typical weathered basement profile reported in literature. The resistivity range (column 2) is the absolute minimum and maximum value found in literature. The resistivity quartile range (column 3) is the range between the first quartile of all of the minimum cited values and the third quartile of all of the maximum cited values in literature. Estimated aquifer characteristics and groundwater potential (ranging from poor to good) of saprolite and saprock from Anudu et al. (2014); and Ebong et al. (2021) are included. Values in bold represent saprolite and saprock of good groundwater potential in at least one of the two studies.

Material	Resistivity absolute range (Ω.m)	Resistivity quartile range (Ω.m)	References
Residual soil	7–10,000	30–1,075	(Adekoya et al., 2019; Adelusi et al., 2014; Aina et al., 1996; Aizebeokhai et al., 2010; Anudu et al., 2014; Bakundukize et al., 2016; Descloitres et al., 2008; Ebong et al., 2021; Elster et al., 2014; Jatau & Bajeh, 2007; Kayode et al., 2016; Kayode, et al., 2022; Kumar et al., 2016; Nyenje et al., 2022; Olayinka & Weller, 1997; Singh et al., 2019; Wekesa et al., 2020)
Saprolite (undefined water content)	4–3,500	15–848	(Adelusi et al., 2014; Aina et al., 1996; Aizebeokhai et al., 2010; Anudu et al., 2014; Descloitres et al., 2008; Ebong et al., 2021; Elster et al., 2014; Foppen et al., 2020; Jatau & Bajeh, 2007; Kayode et al., 2016; Kayode et al., 2022; Olayinka & Weller, 1997; Olorunfemi & Fasuyi, 1993; Zarate et al., 2021)
Saprolite (saturated)	7–700	19–586	Adekoya et al., 2019; Anudu et al., 2014; Bauman et al., 2016; Elster et al., 2014; Kumar et al., 2016; Nyenje et al., 2022)
	Saprolite aquifer characteristics and groundwater potential		
	<10	Clays: limited potential (Anudu et al., 2014; Ebong et al., 2021)	
	21–100	Optimum weathering: good potential (Anudu et al., 2014) Dominantly clay: poor potential (Ebong et al., 2021)	
	101–150	Medium conditions: medium potential (Anudu et al., 2014; Ebong et al., 2021)	
	151–300	Little weathering: poor potential (Anudu et al., 2014) Gravely clay: good potential (Ebong et al., 2021)	
	>300	Negligible potential (Anudu et al., 2014; Ebong et al., 2021)	
Saprock	87–infinity	175–2,979	(Adekoya et al., 2019; Aizebeokhai et al., 2010; Anudu et al., 2014; Descloitres et al., 2008; Ebong et al., 2021; Kayode et al., 2022; Kumar et al., 2016; Olayinka & Weller, 1997; Olorunfemi & Fasuyi, 1993; Wekesa et al., 2020; Zarate et al., 2021)
	Saprock aquifer characteristics and groundwater potential		
	<750	High fracture permeability: high potential (Anudu et al., 2014; Ebong et al., 2021)	
	750–1500	Moderately fractured: medium potential (Anudu et al., 2014; Ebong et al., 2021)	
	1500–3000	Fairly low effect of weathering: low potential (Anudu et al., 2014; Ebong et al., 2021)	
	>3000	Little or no weathering: negligible potential (Anudu et al., 2014; Ebong et al., 2021)	
Fresh bedrock	30–infinity	600–infinity	(Adekoya et al., 2019; Adelusi et al., 2014; Aina et al., 1996; Anudu et al., 2014; Bakundukize et al., 2016; Descloitres et al., 2008; Ebong et al., 2021; Groen et al., 2018; Jatau & Bajeh, 2007; Kayode et al., 2016; Kayode et al., 2022)

3.1.1. Alluvium

Alluvium in the riverbed, in which the observed water table rests, varies in composition across a continuum of very loose - loose, moderately well sorted, medium - coarse sand. It is variably interspersed with silt, clay, and gravel layers. As would be expected, the three mature sites have thicker deposits and greater upstream extents of saturated trapped alluvium than the new sites (Table 3). Silt, which typically settles at the end of the rainy season, was observed on the surface of all new sites post-construction.

3.1.2. Residual soil

Residual soil in the riverbanks varies in composition along a clay - loam - sand continuum, varying in density from soft - medium soft clay and loose - dense sand. At Kithunthi, Nthonzweni, and Kyakivandi, the residual soil is predominantly sandy, whilst at Kipico, Ngulai, and Wambiti, it is predominantly clay-rich. The residual soil was only saturated at Kyakivandi (at 0.85 m and 1.2 m bgl).

3.1.3. Saprolite

The alluvium and residual soil are underlain by saprolite. Observed during construction and in observation pits, it comprises soft - moderately stiff sandy clay - clayey silt - clayey sand, and sometimes contains eroded cobbles or boulders of bedrock. Red - orange iron oxide weathering, typical of saprolite, was observed during wall construction at Nthonzweni. The water table observed in the weathered basement was predominantly found here.

3.1.4. Saprock

The expression of the saprock is variable. Parts of the saprock easily lose surface fragments when brushed by hand, crumble in hand, or break when smashed with a hammer. Lower parts of the saprock appear unweathered to sight, being fairly resistant to breaking when hit with a hammer.

The walls at five of the sites: Kithunthi, Kipico, Ngulai, Nthonzweni, and Wambiti are predominantly constructed onto lower saprock. This interpretation is based on hard but slightly weathered rock being observed during wall construction at the new sites. It is also based on resistivity values indicative of saprock (around 232–356 Ω.m) at the known depths of wall construction at the mature sites. Some limited longitudinal seepage beneath the wall at these sites would therefore be expected.

3.1.5. Fresh bedrock

At depth, according to the resistivity profiles, saprock grades into fresh, unweathered bedrock, typically of negligible porosity and hydraulic conductivity (Fig. 2). Kyakivandi appears to be the only site at which the wall is constructed onto fresh bedrock, observed in the field as unweathered, massive outcrops. Shallow longitudinal seepage under this dam wall is therefore not expected.

Table 2
Resistivity and thickness ranges of each material observed in the ERT profiles from 2022 and 2023. The resistivity studied range (row 2) is the absolute minimum and maximum values observed. The resistivity 1st and 3rd quartile (rows 3 and 4) are the first quartile of all of the minimum values and the third quartile of all of the maximum values respectively.

		Geological layer						
		Residual soil	Unsaturated alluvium	Saturated alluvium	Unsaturated saprolite	Saturated saprolite	Saprock	Fresh bedrock
Resistivity (Ω.m)	Literature range (Table)	7–10,000	0.1–800		4–3500	7–700	87-infinity	30–infinity
	Studied range	5–836	5–3000	8–836	28-?	12–1280	42-?	152- > 3000
	1st quartile of minimum	14	12	12	65	18	54	232
	3rd quartile of maximum	467	763	356	–	587	–	3000
	Minimum thickness (m)	0.4	0	0	0	0	0	–
	Maximum thickness (m)	2	1.9	1.9	–	7.2	–	–

Table 3
Approximated thickness of trapped alluvium at the wall and upstream extent of trapped alluvium and specifically saturated trapped alluvium (m) at each of the six sand dam sites based on measurements made in scoop holes and height of the dam wall in 2023 (post-dam construction).

	Kithunthi	Kipico	Ngulai	Nthonzweni	Wambiti	Kyakivandi
Thickness of trapped alluvium at the wall (m)	2.8	2.75	3.3	0.22	1.16	0.66
Upstream extent of trapped alluvium (m)	320	350	250	240	200	200
Upstream extent of saturation in the trapped alluvium (m)	250	70	170	90	150	120

3.2. Lateral seepage

Lateral seepage has been defined as that flowing between the alluvial aquifers and weathered basement aquifers via the riverbanks when the water tables are hydraulically connected. Variations in resistivity and water levels between the riverbed and riverbanks can help indicate levels of potential lateral seepage from the alluvial aquifers into the adjacent weathered basement.

3.2.1. Geophysics

More extensive low resistivity material across the riverbeds and adjacent riverbanks is observed in the upstream compared to downstream profiles, the latter of which are outside the extent of accumulated trapped alluvium (Fig. 5). This is likely attributed to the greater saturated thickness of trapped alluvium upstream and a subsequently greater potential for lateral seepage. Very low resistivity values in the riverbanks at Ngulai and Kithunthi, however, may, in part, be attributed to clay (Fig. 5b, 6a). This is supported by augering to 2.1 m bgl, which showed the topsoil and saprolite to be variably composed of sand, silt, and clay. Beyond the upstream extent of saturated trapped alluvium at Kipico there are very high resistivity signatures in the riverbed and riverbanks of profiles 3 and 5. This suggests an absence of saturated alluvium and therefore limited seepage compared to profile 2 just upstream. Whilst lower resistivity material is observed around the upstream extent of profile 4 (perpendicular to the dam wall) compared to just upstream, high IP signatures confirm that this is likely attributed to clay rather than water content (Fig. 8c).

There is more extensive low resistivity material in the riverbanks in the upstream profiles at Kithunthi (Fig. 6a) and Ngulai (Fig. 5a, b) (>8 Ω.m) compared to Kipico (Fig. 6b) (>28 Ω.m). This suggests higher water storage at the former two. Low resistivity signatures in the riverbed continue into both riverbanks at Kithunthi and Ngulai upstream, suggesting potential lateral seepage. This may not be the case at Kipico, where the lowest resistivities are confined to the riverbed.

At the new sites there is slightly less extensive low resistivity material in the riverbeds and surrounding weathered basement than at Kithunthi and Ngulai, but slightly more than was observed pre-construction. This is likely, in part, due to less time elapsing since construction, allowing less lateral seepage.

3.2.2. Hydraulic gradients

Water levels elevations taken at Kithunthi (20 m upstream), Kipico (9 m upstream), Ngulai (150 m upstream), and Kyakivandi (45 m upstream) are higher in the centre of the riverbed compared to those in the riverbanks. Horizontal hydraulic gradients and therefore seepage away from the riverbeds exist as a result of the groundwater mound created by recharge of the alluvium (Fig. 7). This is in comparison to Ngulai (9 m upstream), where the water level elevation in the riverbed is lower than in the riverbank, with a hydraulic gradient into the riverbed.

There are limited wells for water measurements in the riverbanks, with no water levels being available further than 17 m from the riverbed edge. No water level measurements are available in the riverbanks at Nthonzweni or Wambiti.

3.3. Sub-vertical seepage

Sub-vertical seepage has been defined as the sub-vertical component of lateral loss from sand dams into the surrounding weathered basement aquifer via the base of the riverbed. This occurs whether or not the sand dam is connected to the water table in the weathered basement. Variations in resistivity beneath the alluvial aquifers, as a result of water content and geology, as well as water levels in the trapped alluvium help to suggest variable levels of potential sub-vertical water seepage.

3.3.1. Geophysics

When comparing inversion profiles pre- and post-construction at the three new sites, a slight decrease in resistivity is observed in and directly below the trapped alluvium during the studied dry season. This is interpreted to be because of a slight increase in water content. This suggests some sub-vertical seepage into the weathered basement because of increased water storage in the trapped alluvium. Such a change was not observed in downstream profiles. This is supported by IP inversions. At Nthonzweni, in 2022, there was a high chargeability signature beneath the riverbed. In 2023 this signature was lower and may suggest a slight increase in water content in the subsurface.

The resistivity of material underlying the alluvial aquifers varies

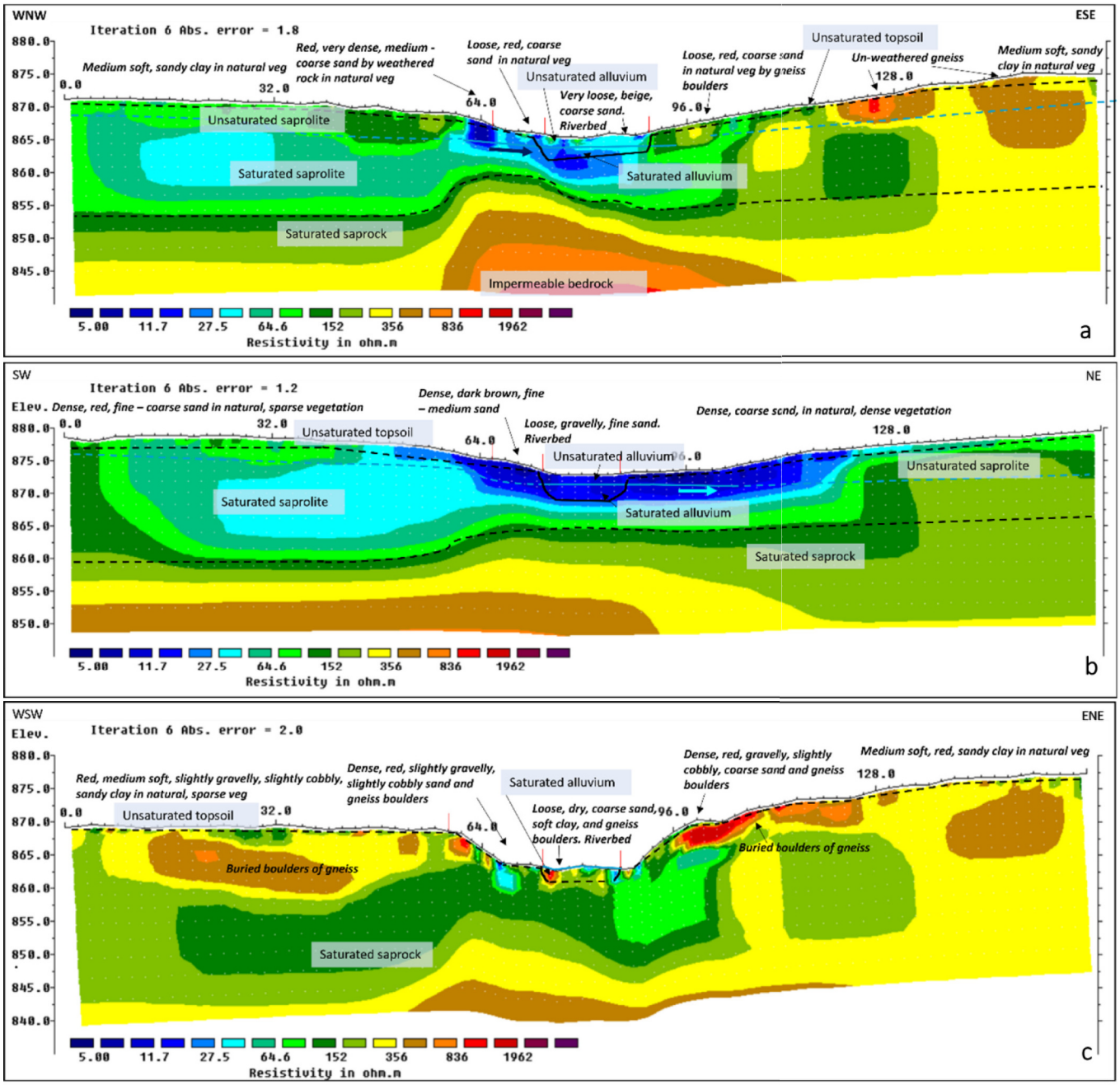

Fig. 5. ERT profiles parallel to the dam wall at Ngulai 2022 (a) 9 m upstream, (b) 150 m upstream, (c) 13.5 m downstream. Profiles include surface observations in italics, with each change separated by red markers; observed and estimated layer boundaries in solid and dashed lines respectively (black for geological layers and blue for water table); and interpreted layers in boxes. Sub-surface arrows indicate estimated flow direction. (For interpretation of the references to colour in this figure legend, the reader is referred to the web version of this article.)

between Wambiti (Fig. 8a) and Kyakivandi (Fig. 6c), and the other four sites. At the former two sites, the alluvium upstream of the dam wall is consistently underlain by saprock and fresh bedrock of 152- > 3000 Ω.m at 0–3.05 m bgl. This is observed in inversion profiles and in the field as outcrops of unweathered gneiss and schist in the riverbed. The change in resistivity values with depth is relatively sudden at these two sites. This indicates a relatively rapid change in basement properties over a small vertical distance. Resistivities in the crystalline bedrock can vary because of fracturing in the saprock. This is especially evident in the perpendicular profile, Fig. 8a. This indicates some potential sub-vertical seepage from the alluvium into the crystalline basement at these sites. The parallel profiles conversely show more extensive, shallow fresh bedrock, indicating localised areas of impeded sub-vertical seepage (Fig. 6c).

The alluvial aquifers at the four remaining sites are consistently underlain by saprolite of 18–232 Ω.m (Fig. 8b,c). There is negligible unweathered rock observed in the riverbeds of Kithunthi, Kipico, and Nthonzweni. The change in resistivity values with depth at these four sites is generally more gradual than that seen at Wambiti and Kyakivandi, indicating a slower transition in basement properties and a greater depth of weathering. Higher potential sub-vertical water seepage is expected at these sites due to an absence of shallow unweathered bedrock. The relative lateral homogeneity in the perpendicular profiles of these sites is interpreted to be because of continuously saturated saprolite and saprock. Low resistivity and a general absence of high IP signatures below the depth of alluvium, alongside field

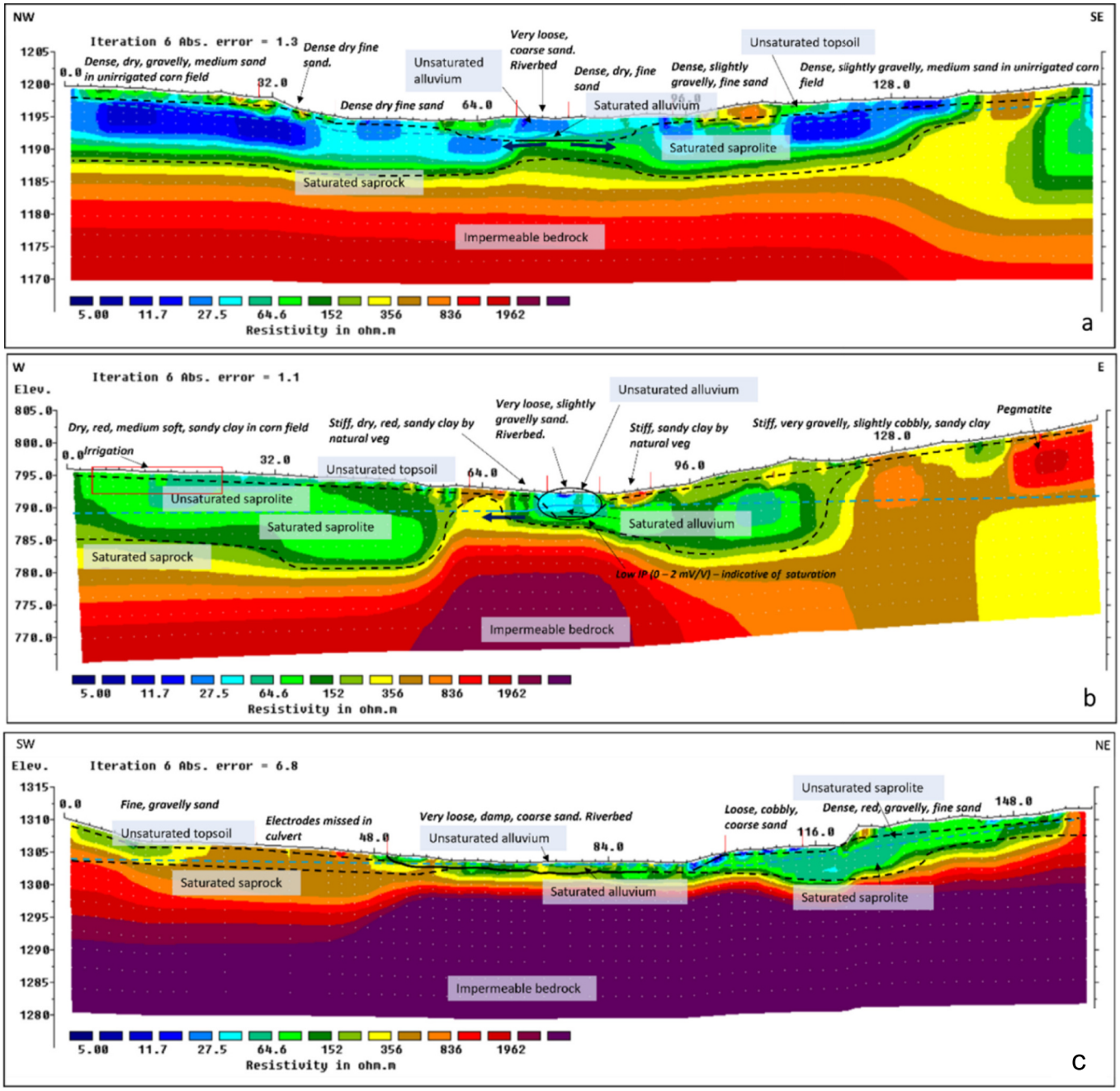

Fig. 6. ERT profiles parallel to the dam wall at (a) Kithunthi 20 m upstream (2022), (b) Kipico 9 m upstream (2022), (c) Kyakivandi 140 m upstream (2023). Profiles include surface observations in italics, with each change separated by red markers; observed and estimated layer boundaries in solid and dashed lines respectively (black for geological layers and blue for water table); and interpreted layers in boxes. Arrows indicate estimated flow direction. (For interpretation of the references to colour in this figure legend, the reader is referred to the web version of this article.)

observations, suggest an absence of an impermeable very clay-rich layer which would impede saturated flow.

3.3.2. *Water levels*

The water levels in the alluvium get deeper further upstream at the new sites and Kipico. Conversely, at Ngulai and Kithunthi, the water levels are deepest at the wall. This is potentially due to handpump abstraction here, which was not occurring at the other four sites. Water levels are generally shallower (Table 4) and alluvium thinner (Table 4) at the new sites.

Deeper water levels at Kipico and higher resistivity values in the regolith compared to other sites could be attributed to a lower water content in the regolith due to a faster rate of seepage into the surrounding aquifer. This may be due to greater hydraulic conductivity between the regolith and crystalline basement. Conversely, at Kithunthi and Ngulai, the measured water levels are comparatively shallower, and resistivity values comparatively lower, suggesting greater volumes of water stored in the regolith and a slower rate of seepage. This would be characteristic of a lower hydraulic conductivity between the regolith and crystalline basement.

3.4. *Longitudinal seepage*

Longitudinal seepage has been defined as shallow groundwater flow under or around the dam wall from the upstream aquifer and emerging into the alluvial riverbed downstream. The difference in resistivity and

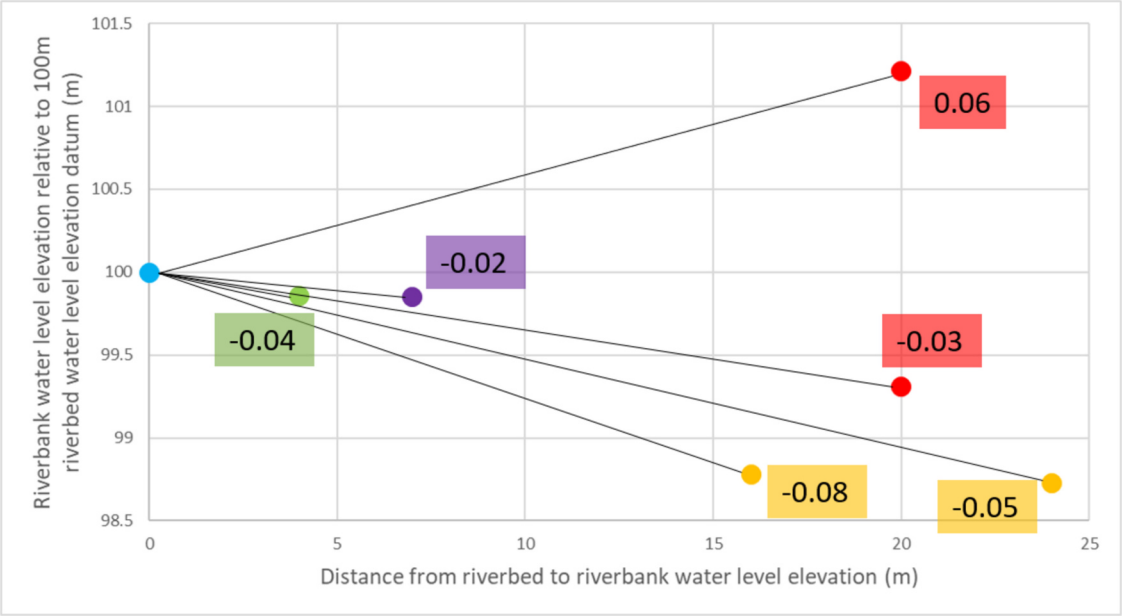

Fig. 7. Riverbank water level elevations relative to a 100 m riverbed water level elevation datum taken at Kithunthi (green), Kipico (purple), Ngulai (red), and Kyakivandi (orange) upstream with the distance between the water level measurements in the riverbanks and riverbed (blue) along the x axis. Hydraulic gradients are in the coloured boxes next to each water level elevation. See Supplementary Material for data. (For interpretation of the references to colour in this figure legend, the reader is referred to the web version of this article.)

water levels in the riverbed upstream and downstream of the dam wall can help indicate variable levels of potential longitudinal seepage from the alluvial aquifers.

3.4.1. Geophysics

At the three mature sites, greater thicknesses of low resistivity material (minimum of 5 Ω.m) are observed upstream compared to downstream during the studied dry season. Downstream, low resistivity values are less extensive and reach a minimum of 12 Ω.m (Fig. 5c, 8b, c). This indicates increased water storage upstream and limited longitudinal seepage under or around the dam wall especially at Kithunthi and Kipico. Low resistivity material directly downstream of the dam wall at Ngulai in connectivity with that upstream suggests greater longitudinal seepage here, supported by field observations of surface water pooling up to 0.9 m deep on the downstream side of this dam wall.

At the new sites, pre-construction, low resistivity signatures (minimum of 8 Ω.m) were observed in the upstream and downstream riverbeds. Post-construction, more extensive and slightly lower resistivity material was observed upstream compared to downstream (minimum of 8 Ω.m and 12 Ω.m respectively). This is likely due to the thin build-up of water saturated alluvium upstream. The amount of low resistivity material downstream generally decreased post-construction, likely because of the excavation and construction of the dam wall onto the saprock or unweathered bedrock preventing groundwater losses through the saprolite and alluvium. This again indicates that the dam walls are leading to an accumulation of saturated alluvium upstream, whilst limiting longitudinal seepage to the downstream alluvium.

3.4.2. Hydraulic gradients

Water levels at each site are higher upstream compared to downstream, with hydraulic gradients in the alluvium existing in a downstream direction. This indicates the potential for longitudinal seepage beneath and/or around the dam wall at all sites, depending on the quality of the seal between the dam wall and the bedrock and the degree of weathering of the bedrock. Hydraulic gradients downstream are greater than those upstream at all sites (Table 5). Assuming continuity of flow between up- and downstream of the sand dam, this increase may be due to a reduced cross-sectional area of flow downstream, due to the reduced saturated thickness and/or riverbed width downstream. At Kyakivandi, where the base of the dam wall is constructed onto unweathered bedrock and therefore loss under the wall is concluded to be absent or very minimal, groundwater loss around the sides of the wall may be occurring. This is likely as bedrock was observed 3.7 m below the top of the wingwall, with part of the wingwall therefore being grouted onto weathered rock.

3.5. Revised conceptual sand dam model

The results help to conceptualise the studied sand dams and to answer the question of whether the alluvial aquifers are in hydraulic connectivity with the surrounding weathered basement (existing as MAR structures) (Fig. 9a) or are shallowly underlain by unweathered bedrock (existing more as storage structures) (Fig. 9b). An additional model where the alluvial aquifer is directly surrounded by low permeability clay (existing as perched aquifers, as described in some literature) is included for comparison (Fig. 9c).

The available evidence suggests that sand dams exist along a continuum of connectivity with their surrounding aquifer, functioning predominantly as MAR structures (Fig. 9a). Kithunthi, Kipico, Ngulai, and Nthonzweni were fully characterised as such. Greater hydraulic connectivity and subsequent seepage between the alluvium and surrounding weathered basement exist here. This is due to the alluvium being directly underlain by saprolite or saprock of low - high permeability, with deeper unweathered bedrock, and a connectivity between the water table in the alluvium and surrounding weathered basement. The low - moderate resistivity values of the saprolite and saprock, which gradually increase with depth, suggest a gradual change in the properties of the weathered basement, rather than a sharp no-flow boundary, as would be expected in the perched aquifer model (Fig. 9c). Where riverbeds are underlain by thick layers of saprolite or saprock, water will be lost from the riverbed, recharging the surrounding layers to an extent. Such sites may be recognised pre-construction as having negligible unweathered rock in the riverbed as was the case at Kithunthi, Kipico, and Nthonzweni. Wambiti and Kyakivandi also show recharge behaviour across parts of the sites. Saturation was interpreted between the alluvium and underlying basement during the time of this study (mid-dry

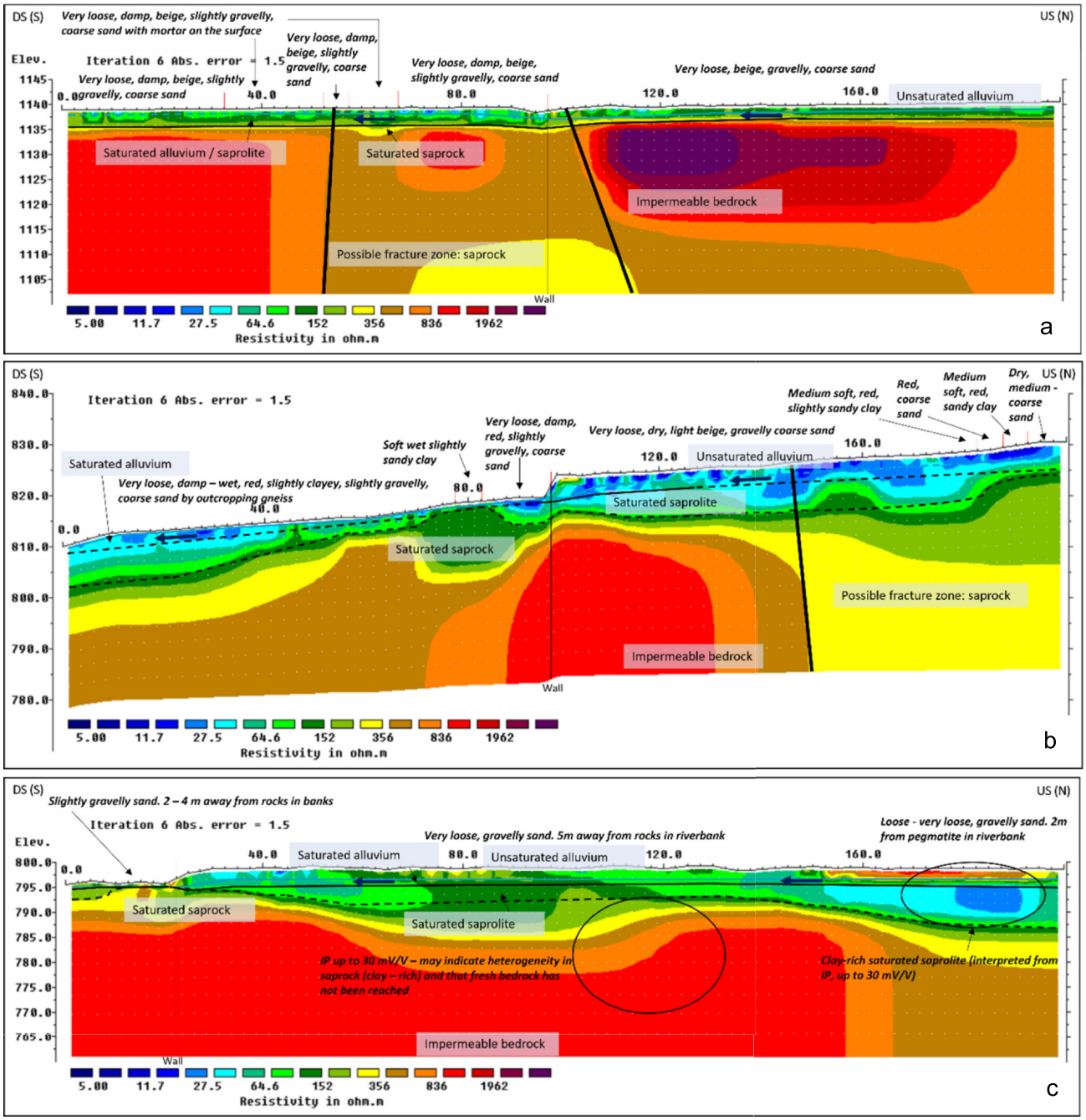

Fig. 8. ERT profiles perpendicular to the dam wall from downstream to upstream (2022) at (a) Wambiti, (b) Ngulai, (c). Profiles include surface observations in italics, with each change separated by red markers; observed and estimated layer boundaries in solid and dashed lines respectively (black for geological layers and blue for water table); and interpreted layers in boxes. Arrows indicate estimated flow direction. (For interpretation of the references to colour in this figure legend, the reader is referred to the web version of this article.)

season). It is possible, however, that the inversion profiles and water level measurements would be different at different times of the year. At the end of the dry season, for example, if the water level has dropped below the base of the alluvial aquifer, the alluvium will no longer be in hydraulic connectivity with the underlying basement. An unsaturated layer would then exist.

Some of the sites (Wambiti and Kyakivandi) locally show characteristics of storage structures, with an impediment of sub-vertical seepage (Fig. 9b). The existence of lateral seepage, however, means that a MAR function still somewhat exists. Fig. 9b represents a more limited hydraulic connectivity between the alluvium and surrounding basement due to the alluvium being underlain at shallow depths by unweathered bedrock. This could occur because of fluvial flows having eroded much of the saprolite and saprock. The alluvial aquifers at Wambiti and Kyakivandi are underlain by either fractured saprock or fresh bedrock, the former which will enable localised seepage. In areas characterised as Fig. 9b, lower sub-vertical seepage is expected than those characterised as Fig. 9a due to the generally lower saturated thickness and hydraulic conductivity of the underlying material. Sites, such as these, characterised as providing better storage potential may be recognised pre-construction as generally having more outcropping unweathered rock in the riverbed and riverbanks.

Some literature portrays sand dams as perched aquifers (Fig. 9c). No studies have formally identified evidence of such classification of sand

Table 4
Range of water depths (m bgl) from the wall to 400 m upstream at each site measured in 2022 (white) and 2023 (grey).

Distance upstream (m)		Mature sites						New sites					
		Kithunthi		Kipico		Ngulai		Nthonzweni		Wambiti		Kyakivandi	
	Year	22	23	22	23	22	23	22	23	22	23	22	23
10	Water depth (m bgl)	1.87	0.95	2.10	2.19	1.40	1.30		0.20	0.8	0		0
50		1.90							0.05	0.45		0.30	0
100		1.65	1.03	1.98	2.20		1.45	0.36	0.37	0.5	0.31	1.05	0.25
150		1.03				1.2	1.09		0.97	0.48		0.37	
200			0.66		2.30		1.07		0.45	0.9	0.32		0.36
300			0.60		2.30		0.92		0.48		0.51		0.55
400					2.84		0.95		1.15	0.55	0.47		0.51

Table 5
Horizontal hydraulic gradients in the upstream and downstream riverbed at each site. See Supplementary Material for data.

	Kithun-thi	Kipico	Ngulai	Nthonz-weni	Wambiti	Kyakivandi
Up-stream hydraulic gradient	−0.004	−0.005	−0.008	−0.004	−0.002	−0.002
Down-stream hydraulic gradient	−0.013	−0.009	−0.017	−0.005	−0.003	−0.015

dams. Similarly, this work did not uncover evidence that any of the studied sites were behaving in this way. To the depth at which dug holes could assess the subsurface before collapse or water infiltration, there was no thick impermeable clay layer. Neither was there geophysical evidence of a continuous low permeability layer beneath the alluvial aquifers underlain by an unsaturated layer. Having said this, due to an abundance of low resistivity material in certain profiles (Fig. 5b, 6a) it is possible: a.) that a thicker clay layer exists beyond the depth of the dug holes and b.) for a thin, low permeability layer to not be apparent on the inversion profiles. At other sand dam sites, where a thick layer of clay may underlie and surround the alluvium, sub-vertical and extensive lateral flow may be impeded, enabling some sites to exist more like perched aquifers.

4. Discussion

More accurate conceptualisation of seepage from sand dams to the surrounding aquifer is important for maximising the potential impact that sand dams can have on small-scale sustainable water use in drylands (Eisma and Merwade, 2021; Ndekezi et al., 2023; Quinn et al., 2019; de Trincheria et al., 2018; Viducich, 2015). The integration of ERT and water level measurements provide evidence of the relative importance of lateral and longitudinal water seepage from the alluvial aquifers into the weathered basement. It does this by identifying areas of saturated weathered basement and the nature of material underlying the alluvial aquifers.

The results highlight the effectiveness of alluvial aquifers in ephemeral rivers across drylands as local recharge structures, whilst low resistivity values within the upstream trapped alluvium indicates their storage potential. Whilst previous studies have found that focussed recharge can be substantial, (Constantz et al., 2002), diffuse recharge is generally concluded to be of greater importance in African drylands (Butterworth et al., 1999; Sorensen et al., 2024). For example, Sorensen et al. (2024) found that at one ephemeral stream, despite retention of water during the monsoon, focussed recharge was still relatively unsubstantial due to low permeability of the riverbed. This highlights that whilst sand dams and other similar structures from which water may be lost, such as check dams and infiltration ponds, can contribute to recharge, the contributed volume, especially due to the small-scale nature of sand dams is likely minimal.

4.1. Lateral seepage

Lateral seepage will likely occur at sand dams, especially at the start of the dry season when the groundwater mound in the alluvium has been replenished. The water level measurements (Fig. 7) suggest there is generally a lateral hydraulic gradient from the alluvial aquifers into the adjacent weathered basement. This is generally consistent with the findings of Quinn et al. (2019), who conducted water balances at two of the mature sites in this study. They found one to lose water throughout the dry season, whilst the other initially gained water, before losing water around 1-month into the dry season.

Further from the riverbed, the low resistivity values at higher elevations (Fig. 6a) may represent a reversal back to the natural hydraulic gradient towards the riverbed. This would be consistent with the findings of Borst and Haas (2006), Hoogmoed et al. (2007), and Strohschein (2016). The lack of water level measurements further into the riverbanks limits this interpretation. Borst and Haas (2006) and Hoogmoed et al. (2007) monitored water levels in 21 piezometers in the riverbed and riverbanks (up to approximately 30 m from the riverbed) in the dry season and found that heads in the alluvium were higher than those in the adjacent riverbanks. This resulted in lateral seepage from the groundwater mound (created from recharge in the alluvium) into the weathered basement until equilibrium was met. Groundwater heads further into the riverbank were found to be higher than those close to the riverbed, concluding that groundwater flow was orientated towards the riverbed outside the zone of influence of sand dams.

There is lower resistivity material in the riverbeds and riverbanks within the upstream extent of saturated trapped alluvium compared to downstream and beyond the upstream extent of saturation. This supports a hydraulic connection between the alluvium and weathered basement. This is consistent with what Hoogmoed et al. (2007) and Strohschein (2016) found. In the upstream alluvium they recorded higher groundwater levels in the riverbed compared to the riverbanks but higher levels in the riverbanks compared to the riverbeds downstream of the dam walls. This resulted in groundwater flows orientated towards the riverbanks and riverbeds, respectively.

Other results from the current study are less conclusive about the

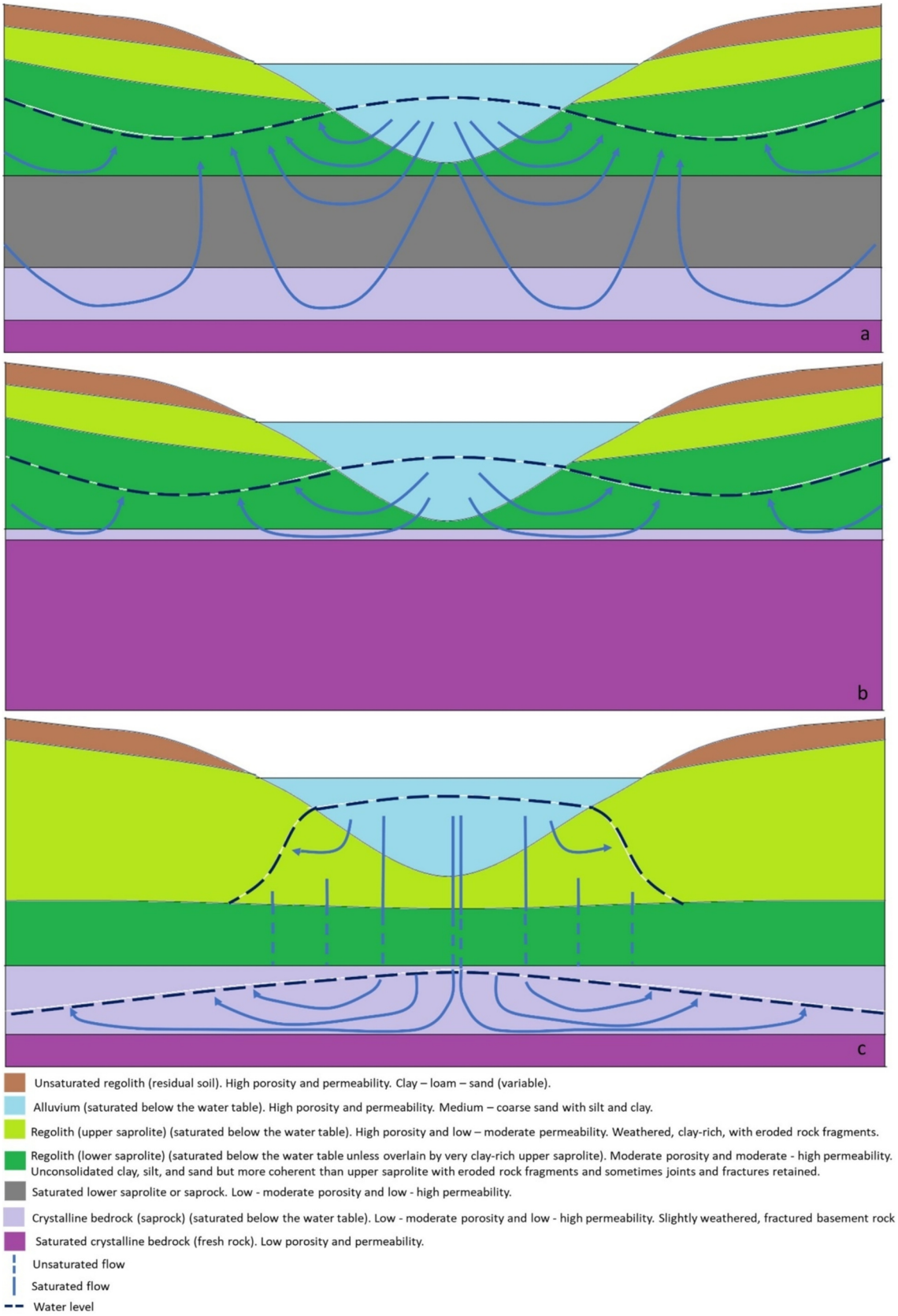

Fig. 9. Conceptual models of a sand dam alluvial aquifer functioning as (a) Managed Aquifer Recharge (MAR), (b) storage structures, (c) perched aquifers.

impact that the alluvial aquifers have on lateral seepage. The resistivity signatures in the riverbanks at the new sites have not extensively changed one-year post-construction and continuity of low resistivity material across the riverbed and riverbank was already seen at Wambiti pre- construction, where no trapped alluvium had accumulated. This may be due to seepage from the pre-existing riverbed. Furthermore, similarly low resistivity signatures are seen in the riverbanks of some of the new and mature sites and in the riverbanks upstream and downstream. This indicates that low resistivity signatures in the riverbanks are likely not solely because of saturation, and/or that saturation in the riverbanks is not solely because of lateral water seepage from the alluvial aquifers. These results highlight the challenges of ERT in investigating seepage, as other variables (apart from just saturation) can influence resistivity signatures. Furthermore, as ERT is difficult to use at rocky sites (as evidenced from site selection during this study), it is suggested that other geophysical techniques, such as seismic could be used to encompass a greater range of sites. This would help to confirm whether the rockier sites in this study are more successful at storing water.

Installing piezometers in the weathered basement is challenging and was not attempted in this study. However, with more time and resources, installing a series of piezometers in the riverbanks as Hoogmoed et al. (2007) did, and/or using environmental tracers would enable greater confidence in lateral seepage interpretations and improved conclusions regarding surface-groundwater interactions. Dashora et al. (2018) for example concluded that at one site there was no hydraulic connection between the surface and groundwater level because the infiltration rate did not diminish sharply during periods of high groundwater levels or rise quickly when levels declined.

4.2. Sub-vertical seepage

Water stored in the trapped alluvium behind the dam walls at each of the sites has produced alluvial aquifers, underlain directly by either saprolite, saprock or fresh bedrock. More sub-vertical seepage is expected to occur at sites continuously underlain by saprolite (as long as it is not very clay-rich), as opposed to those underlain by predominantly fresh bedrock due to higher hydraulic conductivity at the former.

Some sub-vertical seepage is expected to occur at all the studied sand dam sites through the underlying saprolite or saprock. Whilst saprock is typically permeable, its porosity is lower than saprolite, resulting in lower storage capacity but greater transmissivity than the upper saprolite, with evidence of ephemeral rivers losing water when underlain by saprock (Bakundukize et al., 2016; Kumar et al., 2016; Zarate et al., 2021). Upper saprolite typically has lower transmissivity, inhibiting flow if very clay-rich (Olorunfemi and Fasuyi, 1993). Whilst low resistivity values suggest that some clay-rich material exists, such inhibition of flow does not appear to occur at any of the studied sites as the majority of the observed saprolite is not exceptionally clay-rich. This will enable some sub-vertical seepage of water from the alluvial aquifers at all studied sites in at least some locations. Whilst more clay-rich material may be present at greater depths, unless this is continuous beneath the alluvium, some seepage will likely still occur.

Several ERT studies in crystalline basement terrain with similar inversion profiles to those in the current study have made similar interpretations based often on more constraining data (Aizebeokhai et al., 2010; Elster et al., 2014; Nyenje et al., 2022). Aizebeokhai et al. (2010) interpreted the lowest resistivity layers in their profiles as saprolite (4–50 Ω.m and 1–100 Ω.m respectively), being underlain by saprock (of higher resistivity than the saprolite but lower than the bedrock), with groundwater saturating both layers. Kumar et al. (2016) also identified weathered and fractured saturated granite up to 500 Ω.m. Finally, sub-vertical anomalies in inversion profiles observed by Groen et al. (2018), similar to Fig. 8a were interpreted as fracture zones, which would allow sub-vertical seepage.

A study should be conducted once the new sand dams have reached maturity to collect water level measurements in the riverbed. This would help to confirm whether the water levels in the alluvium at sites characterised as Fig. 9b (storage) are shallower than those at sites characterised as Fig. 9a (recharge) due to lower levels of seepage. It would confirm whether lower levels of seepage are occurring at storage sites or whether areas of fracturing in the saprock and lateral seepage are significant enough to enable equally high levels of seepage as sites characterised fully as MAR.

4.3. Longitudinal seepage

The results confirm that some sand dam walls are constructed onto slightly weathered saprock. This is consistent with the assumptions made by Eisma and Merwade (2021), Gezahegne (1986), Hut et al. (2008), Maddrell (2018), and Quinn et al. (2019). They hypothesised that sand dams are not always constructed onto unweathered material and, therefore, that some seepage under the dam wall is possible. Furthermore, longitudinal hydraulic gradients between upstream and downstream of the dam wall indicate the potential for longitudinal seepage at every site. However, the contrast in shallow resistivity values between generally lower resistivity signatures upstream and higher signatures downstream indicate that minimal longitudinal seepage is generally occurring. This is likely as a result of the dam walls impeding flow and effectively containing water.

4.4. Non-uniqueness of results

Relative levels of water seepage and associated saturation from the alluvial aquifers into the surrounding aquifer is one possible cause of the variable resistivity values observed at the different sites. However, other phenomena apart from water seepage can impact saturation, including rainfall and irrigation (Elster et al., 2014). The northern sites experience similarly high levels of rainfall, whilst the southern sites experience similarly lower levels (Fig. 1). Yet overall lower and higher resistivity sites do not match this distribution of rainfall. Furthermore, no areas of irrigation correspond with the lowest resistivity signatures on the inversion profiles and are sometimes conversely associated with some of the highest resistivity values. These results indicate that no one factor alone can explain the variable resistivity signatures in the inversion profiles.

Furthermore, clay content, mineral salts, porosity, and organic content are other potential causes of low resistivity. Wekesa et al. (2020) found similar expressions of low resistivity material (10–15 Ω.m) in riverbanks as seen in Fig. 5b and Fig. 6a and interpreted these as clay-rich weathered basement, rather than saturated. Whilst some clay-rich material was observed in auger bores and shallow excavations at the studied sites, the upper layers of the saprolite did not generally have a high clay content. It is acknowledged, however, that some local components of the shallow low resistivity signatures within the saprolite may be attributed to clay.

The results from this study and cross-comparison with other studies indicate the uncertainty when it comes to attributing resistivity signatures to water saturation and therefore the interpretation of seepage. IP and field observations can go some way to aiding the interpretation of the resistivity inversion profiles but without boreholes, uncertainty remains. Drilling a borehole in a future study at sand dams would allow a more accurate understanding of the composition of each layer and subsequent conceptual understanding of seepage. It would also enable borehole geophysics to be conducted. Despite this, the ERT profiles have provided a more in-depth understanding of the subsurface below sand dams than has previously been available, valuably adding to the conceptualisation of how sand dams interact with their surrounding aquifer.

4.5. Recommendations

Whilst the ERT results alone are inconclusive as to the extent of water

seepage due to the non-uniqueness of results, combined with field observations and literature, the inversions support the existence of some water seepage laterally and longitudinally at each site. Lateral seepage is seemingly the most notable seepage pathway. The results indicate the positive impact that sand dams can have on local water availability. By constructing dams shallowly underlain by unweathered basement, subvertical seepage will be reduced, hence enabling enhanced water storage in the alluvium. This model would favour abstraction by scoop holes in the alluvial riverbeds. The reverse is true for sites shallowly underlain by weathered basement, where more recharge to the surrounding aquifer is occurring. This model would potentially favour abstraction by deeper boreholes depending on hydrogeological conditions. Whilst lateral seepage in both models supports abstraction by handpumps constructed in the immediate riverbanks, sites underlain shallowly by unweathered basement would enable greater shallow storage here. Identifying sites along this spectrum during site selection would be useful in suggesting how the sand dam will behave. The findings show that a combination of simple surface observations and ERT can help to inform the most appropriate water abstraction method and ensure that sand dams are sited on hydrogeological conditions that match their desired purpose: storage or recharge. This will help to maximise benefits that can be derived from the construction of a sand dam.

5. Conclusion

Combining ERT with water level measurements demonstrates the hydraulic connectivity between sand dams and the surrounding weathered basement. Through the development of conceptual models, it highlights the existence of variable lateral and longitudinal seepage from sand dam alluvial aquifers into the surrounding aquifer. The results suggest that the studied sand dams do not exist as perched aquifers or fully isolated storage structures as suggested in some literature but are generally in greater hydraulic connectivity with their surrounding aquifer. They increase local water storage in the surrounding aquifer as a result of lateral and longitudinal seepage from the alluvium and act as MAR structures, whilst still storing water within the alluvium. By using a combination of ERT and surface observations, it is possible to identify how potential sites for the construction of a sand dam may function along a spectrum of storage to MAR. Identifying which sites may lead to greater or lower levels of seepage is important for understanding how a sand dam will behave and what water resources will be available to local communities.

Funding

This work was funded by Engineering and Physical Sciences Research Council (Grant No: EP/S022066/1). Data supporting this study are openly available in the Cranfield University repository (CORD) at https://dspace.lib.cranfield.ac.uk/handle/1826/20712.

Positionality statement

I, the first author, include this positionality statement as a declaration of my current understanding of who I am and how this may impact my work. I include it to be transparent about my identity and background so that you, as the reader, can know the perspective of the author. I am a British, white, female, early career researcher. Whilst my research is based in Kenya, I had never visited Kenya until 2022. My research is predominantly quantitative, however did include some interviews. My personal and social identities culminated in the privileged position that has allowed me to conduct this research and may have biased some of the research that I have undertaken.

CRediT authorship contribution statement

Hannah Ritchie: Writing – review & editing, Writing – original draft, Visualization, Validation, Project administration, Methodology, Investigation, Formal analysis, Data curation, Conceptualization. **Ian Holman:** Writing – review & editing, Supervision, Methodology, Conceptualization. **Justus Nyangoka:** Resources, Investigation. **Paul Bauman:** Writing – review & editing, Validation. **Alison Parker:** Writing – review & editing, Supervision, Methodology, Funding acquisition, Conceptualization.

Declaration of competing interest

The authors declare that they have no known competing financial interests or personal relationships that could have appeared to influence the work reported in this paper.

Data availability

The datasets analysed during the current study are available in the Cranfield University repository (CORD).

Acknowledgements

The authors greatly appreciate the co-operation and hospitality of Sand Dams Worldwide and Africa Sand Dam Foundation, especially Christine Whinney, Boniface Mavindu, Kyalo Cornelius, Musila Andrew, and Mwanaid during the planning and fieldwork phases of this study. The authors would like to thank Paul Maina and Charles Mwangangi Muriuki, geophysicists with Geoscope Engineering, for their support, expertise, and friendship, which were invaluable during fieldwork. The authors are also grateful to the community members at the study sites, for their insights, patience, food, and joy. The authors would like to thank Jimmy Adcock at Guideline Geo for their invaluable guidance in the interpretation of the geophysics profiles.

Appendix A. Supplementary data

Supplementary data to this article can be found online at https://doi.org/10.1016/j.jappgeo.2024.105542.

References

Adekoya, S.A., Coker, J.O., Oladunjoye, H.T., Adenuga, O.A., 2019. Aquifer characterization of some parts of Ijebu Igbo using electrical resistivity methods. J. Phys. Conf. Ser. 1299. https://doi.org/10.1088/1742-6596/1299/1/012075. Institute of Physics Publishing.

Adelusi, A.O., Ayuk, M.A., Kayode, J.S., 2014. VLF-EM and VES: an application to groundwater exploration in a precambrian basement terrain SW Nigeria. Ann. Geophys. 57 (1). https://doi.org/10.4401/ag-6291.

Aina, A., Olorunfemi, M.O., Ojo, J.S., 1996. An integration of aeromagnetic and electrical resistivity methods in dam site investigation. GEOPHYSICS 61 (2), 349–356. https://doi.org/10.1190/1.1443963. Society of Exploration Geophysicists.

Aizebeokhai, A.P., Olayinka, A.I., Singh, V.S., 2010. Application of 2D and 3D geoelectrical resistivity imaging for engineering site investigation in a crystalline basement terrain, southwestern Nigeria. Environ. Earth Sci. 61 (7), 1481–1492. https://doi.org/10.1007/s12665-010-0464-z.

Anudu, G.K., Essien, B.I., Obrike, S.E., 2014. Hydrogeophysical investigation and estimation of groundwater potentials of the Lower Palaeozoic to Precambrian crystalline basement rocks in Keffi area, north-central Nigeria, using resistivity methods. Arab. J. Geosci. 7 (1), 311–322. https://doi.org/10.1007/s12517-012-0789-x.

Baker, B.H., 1952. Geology of the Southern Machakos District. https://s3-eu-west-1.amazonaws.com/samsamwater1/maps/kenya/geology/Geology+of+the+southern+machakos+district.pdf.

Bakundukize, C., Mtoni, Y., Martens, K., Van Camp, M., Walraevens, K., 2016. Poor understanding of the hydrogeological structure is a main cause of hand-dug wells failure in developing countries: A case study of a Precambrian basement aquifer in Bugesera region (Burundi). J. Afr. Earth Sci. 121, 180–199. https://doi.org/10.1016/j.jafrearsci.2016.05.025.

Bauman, P., Woods, L., Ernst, E., MacLean, D., Shinduke, R., Colin McClymont, A., Theran, A., Naama, 2016. The Geophysical Exploration for Groundwater at the Kakuma Refugee Camp and the Proposed Kalobeyei Refugee Camp in Turkana County. UNHCR, Kenya. https://seg.org/wp-content/uploads/2023/04/Geophysical_Exploration_GW_Kakuma_Kalobeyei_Turkana_County_Rev_0_Final_Report_No_financials_b47aa8bd27.pdf.

Bianchi, M., MacDonald, A.M., Macdonald, D.M.J., Asare, E.B., 2020. Investigating the productivity and sustainability of weathered basement aquifers in tropical africa using numerical simulation and global sensitivity analysis. Water Resour. Res. 56 (9). https://doi.org/10.1029/2020WR027746.

Borst, L., Haas, S.A., 2006. Hydrology of Sand Storage Dams A case study in the Kiindu catchment, Kitui District, Kenya. Master's Thesis. Vrije University. https://www.samsamwater.com/library/L_Borst_SA_de_Haas_-_Hydrology_of_Sand_Storage_Dams_-_A_case_study_in_the_Kiindu_catchment_Kitui_District_Kenya_-_rev1.pdf.

British Geological Survey, 2024. Africa Groundwater Atlas. https://www2.bgs.ac.uk/africagroundwateratlas/index.html. Cited 2 December 2023.

Brunner, P., Therrien, R., Renard, P., Simmons, C.T., Franssen, H.J.H., 2017. Advances in understanding river-groundwater interactions. Rev. Geophys. 55 (3), 818–854. https://doi.org/10.1002/2017RG000556.

Butterworth, J.A., MacDonald, D.M.J., Bromley, J., Simmonds, L.P., Lovell, C.J., Mugabe, F., 1999. Hydrological processes and water resources management in a dryland environment III: Groundwater recharge and recession in a shallow weathered aquifer. Hydrol. Earth Syst. Sci. 3 (3), 345–352.

CHIRPS-GEFS Precipitation Forecasts. (2021), Doi: 10.15780/G2PH2M.

Constantz, J., Stewart, A.E., Niswonger, R., Sarma, L., 2002. Analysis of temperature profiles for investigating stream losses beneath ephemeral channels. Water Resour. Res. 38 (12). https://doi.org/10.1029/2001WR001221.

Dashora, Y., Dillon, P., Maheshwari, B., Soni, P., Dashora, R., Davande, S., Purohit, R.C., Mittal, H.K., 2018. A simple method using farmers' measurements applied to estimate check dam recharge in Rajasthan, India. Sustain. W. Resour. Manag. 4 (2), 301–316. https://doi.org/10.1007/s40899-017-0185-5.

de Trincheria, J., Leal, W.F., Otterpohl, R., 2018. Towards a universal optimization of the performance of sand storage dams in arid and semi-arid areas by systematically minimizing vulnerability to siltation: A case study in Makueni, Kenya. Int. J. Sediment Res. 33 (3), 221–233. https://doi.org/10.1016/j.ijsrc.2018.05.002.

Descloitres, M., Ruiz, L., Sekhar, M., Legchenko, A., Braun, J.J., Kumar, M.S.M., Subramanian, S., 2008. Characterization of seasonal local recharge using electrical resistivity tomography and magnetic resonance sounding. Hydrol. Process. 22, 384–394. https://doi.org/10.1002/hyp.6608.

Dodson, R.G., 1953. Geology of the South-East Machakos Area. Geol. Surv. Kenya Report No. 25. https://docslib.org/doc/6391883/geology-of-the-south-east-machakos-area.

Ebong, E.D., Abong, A.A., Ulem, E.B., Ebong, L.A., 2021. Geoelectrical resistivity and geological characterization of hydrostructures for groundwater resource appraisal in the Obudu Plateau, Southeastern Nigeria. Nat. Resour. Res. 30 (3), 2103–2117. https://doi.org/10.1007/s11053-021-09818-4. Springer.

Eisma, J., Merwade, V., 2020. Investigating the environmental response to water harvesting structures: A field study in Tanzania. Hydrol. Earth Syst. Sci. 24 (4), 1891–1906. https://doi.org/10.5194/hess-24-1891-2020.

Eisma, J., Merwade, V., 2021. A data-driven approach to assessing the impact of water harvesting structures on regional water storage in East Africa. J. Hydroinf. 23 (2), 352–367. https://doi.org/10.2166/hydro.2021.115.

Elster, D., Holman, I.P., Parker, A., Rudge, L., 2014. An investigation of the basement complex aquifer system in Lofa county, Liberia, for the purpose of siting boreholes. Q. J. Eng. Geol. Hydrogeol. 47 (2), 159–167. https://doi.org/10.1144/qjegh2013-068. Geological Society of London.

Ertsen, M.W., Biesbrouck, B., Postma, L., Van Westerop, M., 2005. Community organisation and participatory design of sand-storage dams in Kenya. In: Gossling, T., Jansen, R.J.G., Oerlemans, L.A.G. (Eds.), Coalitions and Collisions. Wolf Publishers, pp. 175–185.

Foppen, J.W., Lutterodt, G., Rau, G.C., Minkah, O., 2020. Groundwater flow system analysis in the regolith of Dodowa on the Accra Plains. Ghana J. Hydrol. Reg. Stud. 28. https://doi.org/10.1016/j.ejrh.2020.100663. Elsevier B.V.

Gezahegne, W., 1986. Sub-surface flow dams for rural water supply in arid and semi-arid regions of developing countries. Master's Thesis. Tampere University. IRC. https://www.ircwash.org/sites/default/files/217-2337.pdf.

Groen, M., Rolf, H., Omiti, A., Cosmas, R., 2018. ISGEAG, 1st Technical Report, Geophysics near Kajido Town. https://www.samsamwater.com/projects/81/data/synthesis_report_Technical_Report_Kajiado_town_AUG2018.pdf.

Hoogmoed, M., Groen, J., Waterloo, M.J., 2007. Analyses of impacts of a sand storage dam on groundwater flow and storage: Groundwater flow modeling in Kitui District, Kenya. Master's Thesis. Vrije University. https://sswm.info/sites/default/files/reference_attachments/HOOGMOED%202007%20Analyses%20of%20Impacts%20of%20a%20Sand%20Storage%20Dam%20on%20Groundwater%20Flow%20and%20Storage.pdf.

Hut, R., Ertsen, M., Joeman, N., Vergeer, N., Winsemius, H., van de Giesen, N., 2008. Effects of sand storage dams on groundwater levels with examples from Kenya. Phys. Chem. Earth 33 (1–2), 56–66. https://doi.org/10.1016/j.pce.2007.04.006.

Issoufou Ousmane, B., Nazoumou, Y., Favreau, G., Abdou Babaye, M.S., Abdou Mahaman, R., Boucher, M., Issoufa, I., Lawson, F.M.A., Vouillamoz, J.M., Legchenko, A., Taylor, R.G., 2023. Changes in aquifer properties along a seasonal river channel of the Niger Basin: Identifying groundwater recharge pathways in a dryland environment. J. Afr. Earth Sci. 197. https://doi.org/10.1016/j.jafrearsci.2022.104742.

Jatau, B.S., Bajeh, I., 2007. Hydrogeological appraisal of parts of Jemaa Local Government area. Res. J. Appl. Sci. 2 (11), 1174–1181 doi=rjasci.2007.1174.1181.

Kayode, J.S., Adelusi, A.O., Nawawi, M.N.M., Bawallah, M., Olowolafe, T.S., 2016. Geo-electrical investigation of near surface conductive structures suitable for groundwater accumulation in a resistive crystalline basement environment: A case study of Isuada, southwestern Nigeria. J. Afr. Earth Sci. 119, 289–302. https://doi.org/10.1016/j.jafrearsci.2016.04.009.

Kayode, O.T., Aizebeokhai, A.P., Odukoya, A.M., 2022. Geophysical and contamination assessment of soil spatial variability for sustainable precision agriculture in Omu-Aran farm, Northcentral Nigeria. Heliyon 8 (2). https://doi.org/10.1016/j.heliyon.2022.e08976.

Koutroulis, A.G., 2019. Dryland changes under different levels of global warming. Sci. Total Environ. 655, 482–511. https://doi.org/10.1016/j.scitotenv.2018.11.215.

Kumar, D., Mondal, S., Nandan, M.J., Harini, P., Sekhar, B.M.V.S., Sen, M.K., 2016. Two-dimensional electrical resistivity tomography (ERT) and time-domain-induced polarization (TDIP) study in hard rock for groundwater investigation: a case study at Choutuppal Telangana, India. Arab. J. Geosci. 9 (5). https://doi.org/10.1007/s12517-016-2382-1.

Loke, M.H., 1999. Electrical imaging surveys for environmental and engineering studies. A practical guide to 2-D and 3-D surveys. https://pages.mtu.edu/~ctyoung/LOKENOTE.PDF.

Lowrie, W., 2007. Fundamentals of Geophysics, Second edition. Cambridge University Press. https://doi.org/10.1017/CBO9780511807107.

MacDonald, A.M., Calow, R.C., 2009. Developing groundwater for secure rural water supplies in Africa. Desalination 248, 546–556. https://doi.org/10.1016/j.desal.2008.05.100.

Maddrell, S., 2018. Sand Dams: A Practical & Technical Manual. https://www.cyrho.com/data/Sand%20Dam%20Manual%20-%20Maddrell.pdf.

Manzi, H., Kuria, D., 2011. The use of satellite images to monitor the effect of sand dams on stream bank land cover changes in Kitui district. J. Agric. Sci. Technol. 13 (2), 132–149. http://journals.jkuat.ac.ke/index.php/jagst/article/view/606.

Matsui, T., Park, S. G., Park, M. K., & Matsuura, S. (2016) Relationship between electrical resistivity and physical properties of rocks, 22nd European Meeting of Environmental and Engineering Geophysics, Near Surface Geoscience 2016. European Association of Geoscientists and Engineers, EAGE. https://doi.org/10.3997/2214-4609.201602101. https://www.researchgate.net/publication/307594447_Relationship_between_Electrical_Resistivity_and_Physical_Properties_of_Rocks.

McCallum, A.M., Andersen, M.S., Giambastiani, B.M.S., Kelly, B.F.J., Ian Acworth, R., 2013. River–aquifer interactions in a semi-arid environment stressed by groundwater abstraction. Hydrol. Process. 27 (7), 1072–1085. https://doi.org/10.1002/hyp.9229.

Middleton, N., Thomas, D., UNEP, 1992. World Atlas of Desertification. Edward Arnold, Sevenoaks. https://digitallibrary.un.org/record/246740.

Modie, L.T., Kenabatho, P.K., Stephens, M., Mosekiemang, T., 2022. Investigating groundwater and surface water interactions using stable isotopes and hydrochemistry in the Notwane River Catchment, South East Botswana. J. Hydrol. Reg. Stud. 40. https://doi.org/10.1016/j.ejrh.2022.101014.

Ndekezi, M., Kaluli, J.W., Home, P.G., 2023. Performance evaluation of sand dams as a rural rainwater conservation and domestic water supply technology in East-African drylands, a case-study from South-Eastern Kenya. Cogent Eng. 10 (1). https://doi.org/10.1080/23311916.2022.2163572.

Neufeld, D.G., Muli, J., Muendo, B., Kanyari, J., 2021. Assessment of water presence and use at sand dams in Kenya. J. Arid Environ. 188. https://doi.org/10.1016/j.jaridenv.2021.104472.

Nissen-Petersen, E., 1997. Water from sand-rivers. In: 23rd WEDC Conference. https://wedc-knowledge.lboro.ac.uk/resources/conference/23/Nissen.pdf.

Nyenje, P.M., Ocoromac, D., Tumwesige, S., Ascott, M.J., Sorensen, J.P.R., Newell, A.J., Macdonald, D.M.J., Gooddy, D.C., Tindimugaya, C., Kulabako, R.N., Lapworth, D.J., Foppen, J.W., 2022. Hydrogeology of an urban weathered basement aquifer in Kampala, Uganda. Hydrogeol. J. 1469–1487. https://doi.org/10.1007/s10040-022-02474-9.

Olayinka, A.I., Weller, A., 1997. The inversion of geoelectrical data for hydrogeological applications in crystalline basement areas of Nigeria. J. Appl. Geophys. 37 (2), 103–115. https://doi.org/10.1016/S0926-9851(97)00005-0.

Olorunfemi, M.O., Fasuyi, S.A., 1993. Aquifer types and the geoelectric/hydrogeologic characteristics of part of the central basement terrain of Nigeria (Niger State). J. Afr. Earth Sci. 16 (3), 309–317. https://doi.org/10.1016/0899-5362(93)90051-Q.

Philipp, A., Grundmann, J., 2013. Integrated Modeling System for Flash Flood Routing in Ephemeral Rivers under the Influence of Groundwater Recharge Dams. J. Hydraul. Eng. 139 (12), 1234–1246. https://doi.org/10.1061/(ASCE)HY.1943-7900.0000766.

Prăvălie, R., 2016. Drylands extent and environmental issues. A global approach. Earth Sci. Rev. 161, 259–278. https://doi.org/10.1016/j.earscirev.2016.08.003.

Quilis, R.O., Hoogmoed, M., Ertsen, M., Foppen, J.W., Hut, R., de Vries, A., 2009. Measuring and modeling hydrological processes of sand-storage dams on different spatial scales. Phys. Chem. Earth 34 (4–5), 289–298. https://doi.org/10.1016/j.pce.2008.06.057.

Quinn, R., Rushton, K., Parker, A., 2019. An examination of the hydrological system of a sand dam during the dry season leading to water balances. J. Hydrol. X, 100035. https://doi.org/10.1016/j.hydroa.2019.100035.

Rusagara, R., Koïta, M., Plagnes, V., Jost, A., 2022. Groundwater recharge pathways to a weathered-rock aquifer system in a dryland catchment in Burkina Faso. Hydrogeol. J. 30 (5), 1489–1512. https://doi.org/10.1007/s10040-022-02506-4.

Ryan, C., Elsner, P., 2016. The potential for sand dams to increase the adaptive capacity of East African drylands to climate change. Reg. Environ. Chang. 16 (7), 2087–2096. https://doi.org/10.1007/s10113-016-0938-y.

Saad, R., Nawawi, M., Tonnizam Mohamad, E., 2012. Groundwater Detection in Alluvium using 2-D Electrical Resistivity Tomography (ERT). Article Electron. J. Geotech. Eng. 17. https://www.researchgate.net/publication/267243392_Groundwater_Detection_in_Alluvium_Using_2-D_Electrical_Resistivity_Tomography_ERT.

Safriel, U., Adeel, Z., Niemeijer, D., Puigdefabregas, J., White, R., Lal, R., Winslow, M., Ziedler, J., Prince, S., Archer, E., King, C., 2005. In: Hassan, R., Scholes, R., Ash, N. (Eds.), The Millennium Ecosystem Assessment Series, Ecosystems and Human Well-Being: Current State and Trends. Island Press.

Scanlon, B.R., Keese, K.E., Flint, A.L., Flint, L.E., Gaye, C.B., Edmunds, W.M., Simmers, I., 2006. Global synthesis of groundwater recharge in semiarid and arid regions. Hydrol. Process. 20 (15), 3335–3370. https://doi.org/10.1002/hyp.6335.

Shao, P., Shang, Y., Hasan, M., Yi, X., Meng, H., 2021. Integration of ERT, IP and SP methods in hard rock engineering. Appl. Sci. 11 (22). https://doi.org/10.3390/app112210752.

Singh, K.K.K., Bharti, A.K., Pal, S.K., Prakash, A., Saurabh Kumar, R., Singh, P.K., 2019. Delineation of fracture zone for groundwater using combined inversion technique. Environ. Earth Sci. 78 (4), 1–12. https://doi.org/10.1007/s12665-019-8072-z.

Sorensen, J.P.R., Gahi, N.Z., Guug, S., Verhoef, A., Koïta, M., Sandwidi, W.J.P., Agyekum, W.A., Okrah, C., George Darling, W., Lawson, F.M.A., MacDonald, A.M., Vouillamoz, J.M., Macdonald, D.M.J., 2024. Groundwater recharge is diffuse in semi-arid African drylands: evidence from highly instrumented observatories. J. Hydrol. 636. https://doi.org/10.1016/j.jhydrol.2024.131227.

Strohschein, P.M., 2016. Exploring the influence of sand storage dams on hydrology and water use [Master's thesis, TU Delft]. TU Delft Repository. https://repository.tudelft.nl/islandora/object/uuid%3Aae7390ad-5884-4c4f-88de-1c6be6fc6be0.

Ulusoy, E., Kadioğlu, Y.K., 2021. Petrography and geochemical decomposition parameters of crystalline rocks; Demirköy intrusive body (DIP), NW Turkey. Bull. Min. Res. Explor. 165, 253–265. https://doi.org/10.19111/bulletinofmre.793795.

UNEP-WCMC, 2007. A spatial analysis approach to the global delineation of dryland areas of relevance to the CBD Programme of Work on Dry and Subhumid Lands. https://resources.unep-wcmc.org/products/789fcac8959943ab9ed7a225e5316f08.

van Loon, A., Droogers, P., 2006. Water evaluation and planning system, Kitui - Kenya WatManSup project (Report No. 2). Future Water. https://futurewater.nl/downloads/2006_VanLoon_FW59.pdf.

Viducich, J.M.G., 2015. Spillway Staging and Selective Sediment Deposition. Unpublished Master's Thesis. Oregon State University. https://ir.library.oregonstate.edu/concern/graduate_thesis_or_dissertations/1z40kx51c.

Watson, A., Kralisch, S., van Rooyen, J., Miller, J., 2021. Quantifying and understanding the source of recharge for alluvial systems in arid environments through the development of a seepage model. J. Hydrol. 601. https://doi.org/10.1016/j.jhydrol.2021.126650.

Wekesa, S.S., Stigter, T.Y., Olang, L.O., Oloo, F., Fouchy, K., McClain, M.E., 2020. Water flow behavior and storage potential of the semi-arid Ephemeral River System in the Mara Basin of Kenya. Front. Environ. Sci. 8. https://doi.org/10.3389/fenvs.2020.00095.

Wright, E.P., Burgess, W.G., 1992. The hydrogeology of crystalline basement aquifers in Africa. Geol. Soc. Spec. Publ. 66, 1–27. https://doi.org/10.1144/GSL.SP.1992.066.01.01.

Yao, Y.Y., Zheng, C.M., Tian, Y., Li, X., Liu, J., 2018. Eco-hydrological effects associated with environmental flow management: A case study from the arid desert region of China. Ecohydrology 11 (1), e1914.

Yifru, B., Kim, M.G., Chang, S.W., Lee, J., Chung, I.M., 2020. Assessment of the effect of sand dam on groundwater level: A case study in Chuncheon, South Korea. J. Eng. Geol. 30 (2), 119–129. https://doi.org/10.9720/kseg.2020.2.119.

Yifru, B.A., Kim, M.G., Lee, J.W., Kim, I.H., Chang, S.W., Chung, I.M., 2021. Water storage in dry riverbeds of arid and semi-arid regions: Overview, challenges, and prospects of sand dam technology. Sustainability 13 (11), 1–17. https://doi.org/10.3390/su13115905.

Zarate, E., Hobley, D., MacDonald, A.M., Swift, R.T., Chambers, J., Kashaigili, J.J., Mutayoba, E., Taylor, R.G., Cuthbert, M.O., 2021. The role of superficial geology in controlling groundwater recharge in the weathered crystalline basement of semi-arid Tanzania. J. Hydrol. Reg. Stud. 36. https://doi.org/10.1016/j.ejrh.2021.100833.

https://dspace.org/

Insights from electrical resistivity tomography on the hydrogeological interaction between sand dams and the weathered basement aquifer

Ritchie, Hannah; Holman, Ian P.; Nyangoka, Justus; Bauman, Paul; Parker, Alison

2024-11-01
Elsevier
https://doi.org/10.1016/j.jappgeo.2024.105542
Ritchie H, Holman I, Nyangoka J, et al., (2024) Insights from electrical resistivity tomography on the hydrogeological interaction between sand dams and the weathered basement aquifer. Journal of Applied Geophysics, Volume 230, November 2024, Article number 105542

Downloaded from a DSpace repository. https://dspace.org/